Article

Pilot-scale implementation of mainstream anammox for municipal wastewater treatment against cold temperature

Qi Zhao [ID], Yongzhen Peng [ID], Jianwei Li, Tipei Jia, Qiong Zhang & Liang Zhang [ID] [✉]

Applying anammox to municipal wastewater treatment promises enormous energy and resource savings; however, seasonally cold conditions pose a considerable challenge, impeding its future applications towards non-tropical regions. In this study, we establish a pilot-scale wastewater treatment plant (50 m³/d) in northern China and implement the partial denitrification coupling anammox process on actual municipal wastewater. Despite seasonal cooling, the nitrogen removal efficiency remains high, ranging from $75.0 \pm 4.6\%$ at 27.8–20.0 °C to $70.4 \pm 4.5\%$ at 10–7.5 °C. This process exhibits remarkable low-temperature tolerance, achieving an in-situ anammox rate of 32.7 ± 4.7 g-N/(m³·d) at 10–7.5 °C and contributing up to $39.7 \pm 6.7\%$ to nitrogen removal. Further ^{15}N stable isotope tracing and kinetic tests reveal that the partial denitrification is capable of supplying increasingly abundant NO_2^- to anammox with decreasing temperature, enabling robust mainstream anammox against seasonal cooling. From 27.8 °C to 7.5 °C, anammox bacteria not only survive but thrive under mainstream conditions, with absolute and relative abundances increasing by 429.1% and 343.5%, respectively. This pilot-scale study sheds fresh light on extending mainstream anammox towards non-tropical regions, taking a necessary step forward toward the sustainability goals of the wastewater treatment sector.

Municipal wastewater treatment stands as a hub in the Water-Energy-Sanitation nexus, fulfilling indispensable roles in progressing towards Sustainable Development Goals[1–4]. Yet, regrettably, there remain considerable concerns surrounding the sustainability of municipal wastewater treatment plants (WWTPs), primarily given their substantial resource and energy consumption, along with the notoriously long carbon footprint[5]. Particularly, when facing influents with low organic carbon levels, most municipal WWTPs compromise on sustainability to secure effluent quality, as evidenced by the widespread use of additional carbon sources in WWTPs worldwide[6–8]. For instance, in China alone, the daily input of additional carbon sources into municipal

WWTPs approaches 10,000 tonnes, highlighting the sustainability challenges the wastewater treatment sector faces.

Anammox is a sustainable biotechnology catalyzed by anammox bacteria (AnAOB) affiliated with the deep-branching phylum *Planctomycetes*[9,10]. AnAOB allows ammonium (NH_4^+) oxidation to molecular nitrogen (N_2) under anaerobic conditions using nitrite (NO_2^-) as the electron acceptor. This autotrophic bioprocess minimizes the requirements for organic carbon and oxygen in nitrogen removal, empowering the development of sustainable wastewater treatment processes[10]. Like other advanced environmental biotechnologies, scaling up anammox under high-temperature conditions is the first step towards global popularization. Over the past decade, mainstream

National Engineering Laboratory for Advanced Municipal Wastewater Treatment and Reuse Technology, Engineering Research Center of Beijing, Beijing University of Technology, Beijing 100124, China. [✉]e-mail: zliang@bjut.edu.cn

anammox has shown promise in tropical and subtropical regions, such as Singapore, Southern China, and Australia, with partial nitrification/anammox (PNA) as the representative process[11–13]. However, its extension towards non-tropical regions remains highly challenging, with seasonally cold conditions posing the most significant obstacle. On the one hand, the doubling time of AnAOB is prolonged with decreasing temperature (exceeding 45 days at 15.0 °C), challenging its retention and enrichment under mainstream conditions[14]. On the other hand, low temperatures easily disrupt the NO_2^- supply for anammox[15–18]. For example, in a two-stage PNA system, an inconspicuous cooling from 17.9 °C to 15.1 °C resulted in a 53% reduction in anammox activity, which was attributed to the deterioration of NO_2^- supply rather than the deactivation of AnAOB[19]. The root cause is that ammonia-oxidizing bacteria (AOB) are more vulnerable to low temperatures than nitrite-oxidizing bacteria (NOB), which implies that during winter operation, NO_2^- from AOB is readily consumed by NOB, preventing the net NO_2^- accumulation under aerobic conditions and limiting the following anammox process[15].

Partial denitrification (PD), an emergent NO_2^- supplier, has garnered growing attention due to its stability[20–22]. Under anoxic conditions, denitrifying bacteria (DB) reduce NO_3^- to NO_2^-, a portion of which serves as the electron acceptor of NH_4^+ oxidation by AnAOB, namely PD coupling with anammox (PDA). The feasibility of the PDA has been demonstrated in laboratory-, pilot-, and even full-scale tests[23–26]. A laboratory-scale test, for example, achieved nitrogen removal efficiency and rate as high as 94.1% and 1.28 g-N/(L·d), respectively, at 25.1–29.4 °C[27]. Besides, the NO_2^- supply of the PD process exhibited remarkable tolerance against adverse conditions, such as fluctuating influent load, soluble chemical oxygen demand (sCOD) to total inorganic nitrogen (TIN) ratio (C/N ratio, 2.5–5.0), pH value (5.0–9.0), and salinity (0.1–10 g/L)[28–31]. Under mainstream conditions, the PDA process potentially offers two critical advantages under seasonally cold conditions. Firstly, it operates on the premise of complete nitrification rather than partial nitrification. Although the PDA may not be as desirable as the PNA regarding aeration savings (with theoretical aeration saving ratios of 47% for PDA versus 63% for PNA)[16], it bypasses the out-selection of NOB, mitigating the risks caused by the deterioration of NO_2^- supply at low temperatures. Secondly, compared to the traditional nitrification-denitrification process, it removes NH_4^+ and NO_3^- concurrently in the anoxic zone, enhancing nitrogen removal capacity while mitigating subsequent nitrification challenges at low temperatures[25]. Nonetheless, to this day, the potential for extending the PD process to non-tropical regions has consistently been overlooked.

Based on the above, we hypothesize that the PDA process is potentially advantageous for mainstream application towards non-tropical regions. Most WWTPs in non-tropical regions experience uncontrollable seasonal cooling and cold conditions (operating temperature below 10 °C). To assess our hypothesis more practically, we designed and established a pilot-scale plant of anaerobic-anoxic-oxic combining with biological contact oxidation (A^2O-BCO) process, treating actual municipal wastewater of 50 m3/d (Fig. 1 and Supplementary Fig. 1). With operating temperature seasonally dropping from 27.8 °C to 7.5 °C, the PDA process was systematically evaluated. The objectives of this study were to (i) investigate the feasibility of mainstream PDA against seasonal cooling and cold conditions of non-tropical regions, (ii) clarify the temperature-dependent kinetics of the PDA process to serve as a reference for future applications, and (iii) understand the responses of AnAOB to natural seasonal cooling.

Results

Nitrogen removal performance of the pilot plant
The pilot plant was operated for 210 days, treating actual municipal wastewater with a low C/N ratio of 3.6 ± 0.7 (Supplementary Table 1). As the air temperature seasonally dropped from 35.0 °C to −17.5 °C, the operating temperature decreased from 27.8 °C to 7.5 °C, dividing the long-term operation into three phases: high temperature (27.8–20.0 °C), seasonal cooling (20.0–10.0 °C), and low temperature (10.0–7.5 °C) (Fig. 2a). In phase I (days 1–87, 27.8–20.0 °C), the pilot plant recovered from a malfunction of the air blower and took 10 days to reach a quasi-steady state. During the following operation, the effluent concentrations of NH_4^+ and TIN were recorded at 0.2 ± 0.3 and 8.2 ± 1.6 mg-N/L, respectively, representing an NH_4^+ removal efficiency (ARE) and TIN removal efficiency (NRE) of 99.4 ± 1.0% and 75.0 ± 4.6%, respectively (Fig. 2b–c). In phase II (days 88–147), although the operating temperature sharply dropped from 20.0 °C to 10.0 °C, nitrogen removal performance remained stable. The effluent concentrations of NH_4^+ and TIN were 0.1 ± 0.2 and 12.1 ± 2.5 mg-N/L, respectively, corresponding to an ARE and NRE of 99.7 ± 0.5% and 72.5 ± 4.8%, respectively. In phase III (days 148–210), the air temperature dropped below 0 °C, and the operating temperature was sustained at a low level of 10.0–7.5 °C. The nitrogen removal performance did not deteriorate as expected. Instead, nearly complete removal of NH_4^+ was achieved, with an ARE as high as 99.9 ± 0.3%. The effluent concentration of TIN was recorded at 12.6 ± 1.6 mg-N/L, corresponding to an NRE of 70.4 ± 4.5%.

Absolute abundance, relative abundance, and spatial distribution of AnAOB
Along with seasonal cooling, we tracked the abundance variations of AnAOB, which not only survived but thrived in the biofilms of the anoxic zone. The absolute abundance of AnAOB was estimated through the qPCR assay targeting the anammox-specific $hzsB$ gene and 16S rRNA gene (Fig. 3a–b). An interesting trend was observed in all four compartments of the anoxic zone: AnAOB abundance significantly increased in the biofilms with seasonal cooling (Supplementary Fig. 2). Taking the second anoxic compartment as an example, the absolute abundance of the 16S rRNA gene ranged from $(6.8 ± 0.4) × 10^8$ to $(1.0 ± 0.1) × 10^9$ copies/g-VSS in phase I. As operating temperature decreased in phase II, it was enriched to $(2.9 ± 0.3) × 10^9$ copies/g-VSS (day 152, 10.6 °C). Over the following low-temperature operation in phase III, the 16S rRNA gene peaked at $(3.6 ± 0.1) × 10^9$ copies/g-VSS (day 205, 8.6 °C) (two-tailed independent t-test, $P = 0.0014$). The variation trend of the $hzsB$ gene closely aligned with that of the 16S rRNA gene. The relative abundance of AnAOB was determined through 16S rRNA amplicon sequencing, which yielded similar results to the qPCR assays (Fig. 3c). *Candidatus Brocadia* as the only detected anammox genus exhibited a significant enrichment from 0.23 ± 0.01% (day 38, 25.3 °C) to 1.02 ± 0.10% (day 205, 8.6 °C) in the anoxic biofilms of the second anoxic compartment (two-tailed independent t-test, $P = 0.001$). The spatial distribution of AnAOB in the anoxic biofilms was characterized using confocal laser-scanning microscopy combining with fluorescence in situ hybridization (CLSM-FISH), which also demonstrated similarity across all four anoxic compartments (Supplementary Fig. 3). Taking the second anoxic compartment as an example, AnAOB primarily occupied the inner-layer biofilms on day 38 (25.3 °C) (Fig. 3g). Interestingly, with seasonal cooling, AnAOB exhibited a noticeable outward extension. By day 205 (8.6 °C), it had spread throughout the outer-layer biofilms and displayed a greater pink fluorescence intensity than the inner-layer biofilms (Fig. 3h). From abundance to morphological distribution, these findings provide compelling evidence for the feasibility of enriching AnAOB during natural seasonal cooling, challenging the prevailing opinion that anammox enrichment is reliant on high temperatures.

Footprint, in-situ reaction rate, and contribution ratio of anammox
In this study, the NH_4^+ removal under anoxic conditions (dissolved oxygen (DO) below 0.01 mg-O_2/L) was identified as the indicator of anammox behavior[10,32], especially considering that our batch tests confirmed that the NH_4^+ concentration variation due to microbial
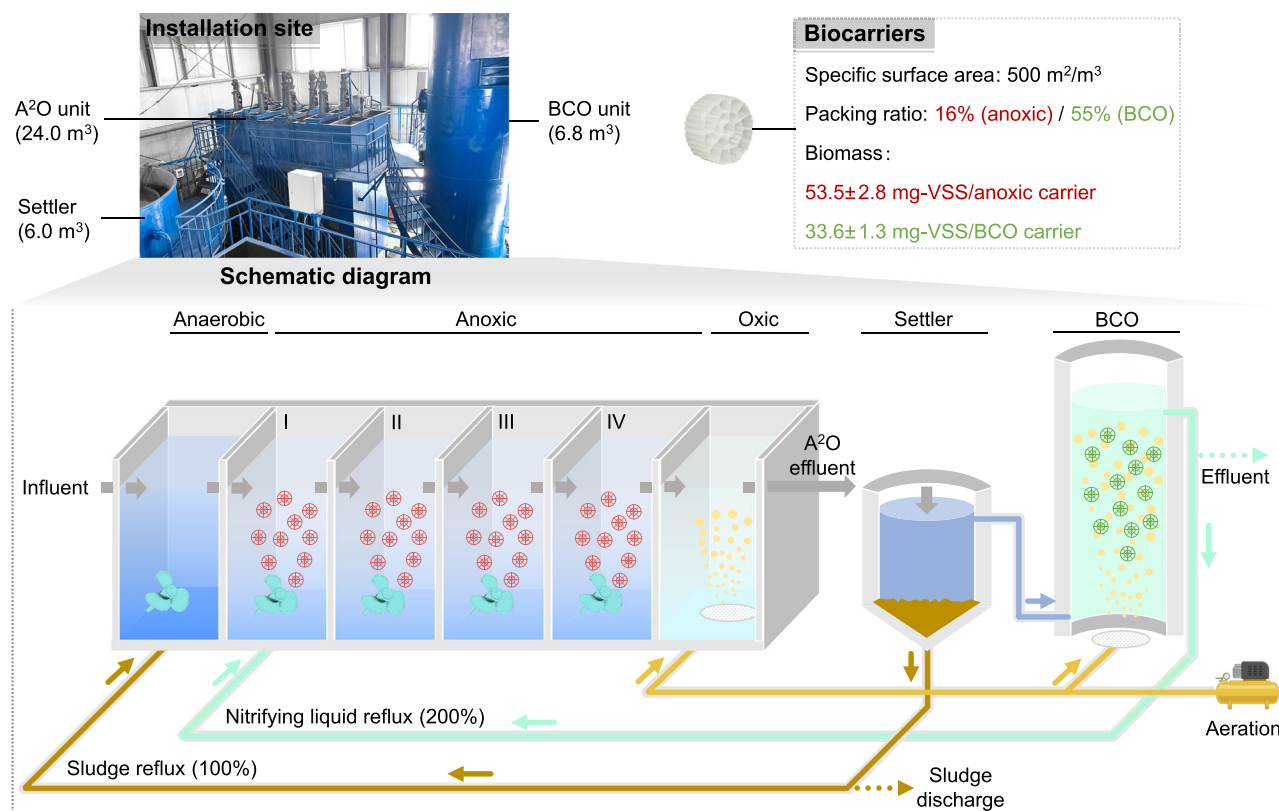
Fig. 1 | Installation site and schematic diagram of the pilot plant of anaerobic-anoxic-oxic combining with biological contact oxidation (A²O-BCO) process and characteristics of biocarriers in the anoxic zone and BCO unit. Figure 1 was created in BioRender. Zhao, Q. (2024) https://BioRender.com/g22j266.

assimilation was at an undetectable level (Supplementary Fig. 4). In phase I, NH_4^+ removal was observed exclusively in the first anoxic compartment, indicating a short anammox footprint (spatial extent of the anoxic zone where anammox activity was detected) (Supplementary Fig. 5). This was primarily attributed to the rapid depletion of NO_3^- at high temperatures, resulting in the absence of NO_3^- and the cessation of the PD process in the following anoxic compartments. The in-situ reaction rate of anammox reached up to 49.4 ± 5.3 g-N/(m³·d) in the first anoxic compartment (Fig. 3d and Supplementary Note 1). Still, its contribution to nitrogen removal was only $11.7 \pm 2.5\%$ due to the limited footprint (Fig. 3e). As the operating temperature gradually decreased in phases II and III, the anammox footprint expanded and covered the entire anoxic zone. In phase III, at low temperatures below 10 °C, the in-situ anammox rate was recorded as 32.7 ± 4.7 g-N/(m³·d). However, due to the extended footprint, the anammox contribution ratio to nitrogen removal increased to $39.7 \pm 6.7\%$ (two-tailed independent t-test, $P = 1.47 \times 10^{-15}$). In addition, it was found that the NO_2^- utilizing ratio (NUR, the ratio of NO_2^- utilized by anammox in total NO_2^- production) significantly increased with seasonal cooling (Supplementary Note 2), from 13.0 ± 2.3 in phase I to $36.6 \pm 5.4\%$ in phase III (two-tailed independent t-test, $P = 3.03 \times 10^{-16}$) (Fig. 3f). The increasingly abundant NO_2^- supply may be a crucial premise underlying the robust mainstream anammox against seasonal cooling.

On days 38 (25.3 °C) and 205 (8.6 °C), we conducted ^{15}N stable isotope tracing tests to confirm the anammox contribution ratio to nitrogen removal. The experimental group ($^{14}NH_4^+$ plus $^{15}NO_3^-$) (Fig. 3i–j) and the control group ($^{15}NH_4^+$ plus $^{14}NO_3^-$) (Fig. 3k–l) yielded similar results. For the samples from day 38, at a test temperature of 25.0 ± 0.5 °C, the $^{29}N_2$ production rates in the experimental and control groups were recorded as 2.00 ± 0.21 and 3.44 ± 0.41 μmol-N_2/(L·h), respectively, corresponding to anammox contribution ratios of 16.9% and 19.9%, respectively (Supplementary Note 3). For the samples from

day 205, at a test temperature of 9.0 ± 0.5 °C, the $^{29}N_2$ production rates were recorded as 1.91 ± 0.23 and 2.60 ± 0.30 μmol-N_2/(L·h) for the experimental and control groups, respectively, representing anammox contribution ratios of 38.1% and 38.3%, respectively. These results aligned well with the long-term in-situ data, reconfirming the higher anammox contribution at lower temperatures.

Temperature-dependent kinetic characteristics of the PDA process

To provide deeper insights into the effects of temperature variations on the PDA process, we established a temperature gradient ranging from 30 °C to 5 °C and conducted a series of kinetic tests. In the light of the modified Arrhenius equation, the activation energy (E_a) and the Q_{10} temperature coefficient between 20 °C and 10 °C ($Q_{10(20-10 °C)}$) for anammox were predicted as 86.9 kJ/mol ($R^2 = 0.996$) and 2.8, respectively (Fig. 4a, Supplementary Note 4, and Supplementary Table 2)[33,34]. The PD process was also assessed, focusing on the NO_2^- production ($NO_3^- \to NO_2^-$) and NO_2^- consumption processes by DB (Fig. 4b–c). The E_a values for NO_2^- production and consumption were predicted as 55.6 kJ/mol ($R^2 = 0.995$) and 105.6 kJ/mol ($R^2 = 0.997$), respectively, with $Q_{10(20-10 °C)}$ coefficients of 2.4 and 4.4. The higher E_a and $Q_{10(20-10 °C)}$ for the NO_2^- consumption process of DB aligned well with previous studies, explaining the NO_2^- accumulation observed under cold conditions (e.g., woodchip bioreactors and sediment-water interface of rivers)[35–38]. These results indicate that the NO_2^- consumption by DB is more vulnerable to temperature variations and will be inhibited more significantly by low temperatures. Specifically, in the temperature range of 30–20 °C, NO_2^- consumption activities (0.30–0.16 g-N/(g-VSS·d)) were significantly higher than NO_2^- production activities (0.25–0.14 g-N/(g-VSS·d)) (two-tailed paired t-test, $P = 0.0361$), suggesting that DB tended to perform complete denitrification without NO_2^- accumulation. In other words, most NO_2^- was
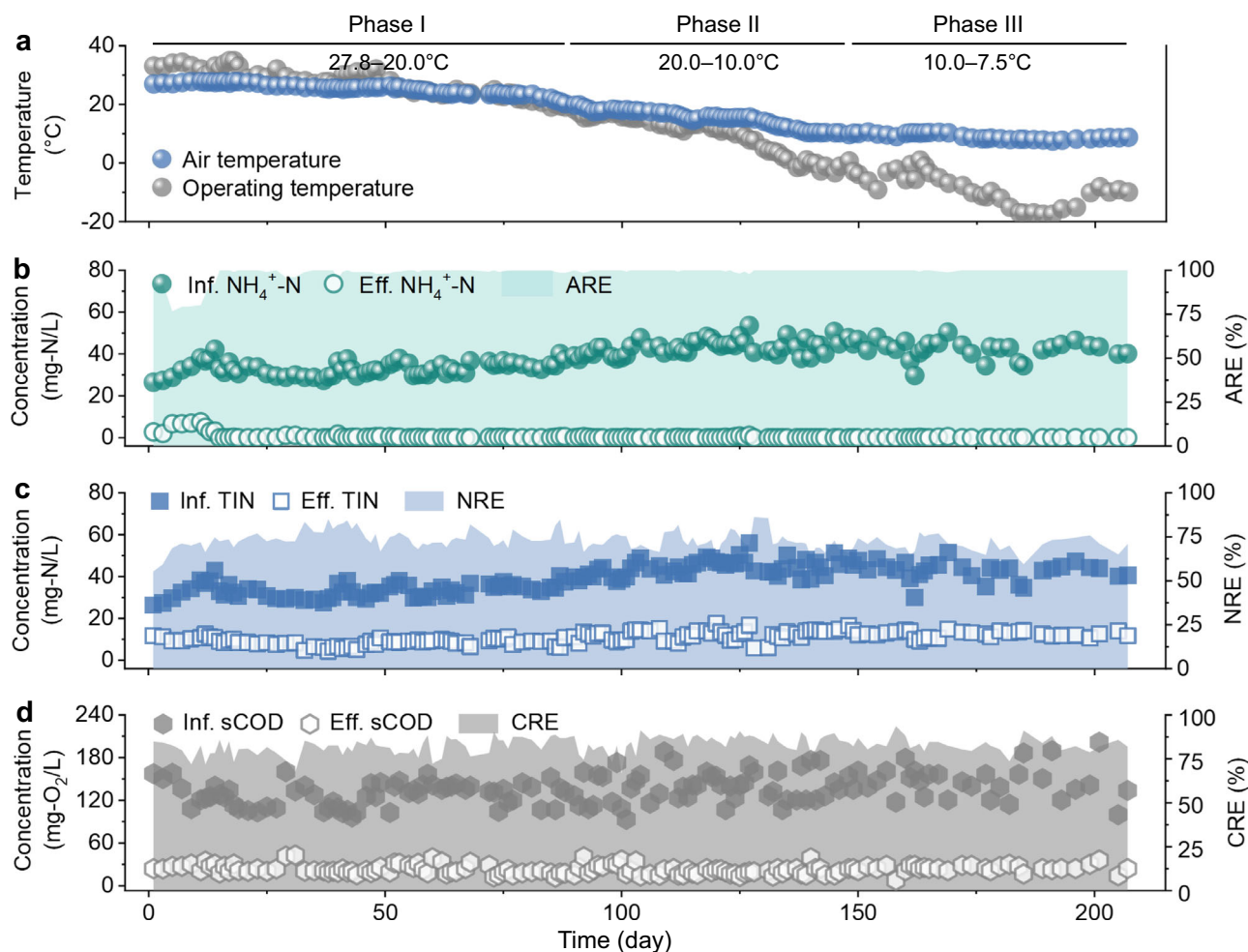
Fig. 2 | Long-term operational performance of the pilot plant. a Air and operating temperatures, recorded around 12:00 PM each day. **b–d** Treatment performance of the nutrients (NH$_4^+$, total inorganic nitrogen (TIN), and soluble chemical oxygen demand (sCOD)), including the influent concentrations, effluent concentrations, and removal efficiencies (NH$_4^+$ removal efficiency (ARE), TIN removal efficiency (NRE), and sCOD removal efficiency (CRE)). Source data are provided as a Source Data file.

consumed through complete denitrification rather than supplied to anammox, which explains the observed low-level NUR ($13.0 \pm 2.3\%$) and limited AnAOB abundance in phase I. However, as the test temperature dropped below 20 °C, NO$_2^-$ production activity surpassed the NO$_2^-$ consumption activity. At 10 °C, the former was 1.6-fold higher than the latter (0.059 ± 0.005 versus 0.036 ± 0.006 g-N/(g-VSS·d)), indicating that 40.1% of the NO$_2^-$ would accumulate and serve as the available substrate for anammox, aligning well with the observed high-level NUR ($36.6 \pm 5.4\%\%$) in phase III. These results suggest a transition in the interactions between DB and AnAOB from competition (for NO$_2^-$ at high temperatures) to collaboration (sharing NO$_2^-$ at low temperatures) and, technically, challenges the prevailing opinion that cold conditions invariably harm the anammox process.

Dynamic succession of bacterial communities and taxonomic origins of key enzymes

16S rRNA amplicon sequencing and metagenomic sequencing were conducted to investigate the dynamic succession of bacterial communities in response to seasonal cooling. Principal coordinates analysis (PCoA) based on the Bray-Curtis distance revealed clear temperature-dependent succession patterns of bacterial communities in both flocs and anoxic biofilms, resulting in two distinct clusters: high temperatures (27.0 °C, 25.3 °C, and 23.0 °C) and low temperatures (16.8 °C, 10.6 °C, and 8.6 °C) (Adonis test, flocs: $P = 0.003$; anoxic biofilms:

$P = 0.001$) (Fig. 5a–b). These findings suggest that seasonal cooling is a core driving force in shaping bacterial communities under mainstream conditions. Regarding anammox, both qPCR and 16S rRNA amplicon sequencing had shown the enrichment of AnAOB in the anoxic biofilms with seasonal cooling (Fig. 3a–c). Metagenomic sequencing on day 205 (8.6 °C) provided deeper insights from the perspective of the taxonomic origins of key enzymes. The anammox-specific *hzs* gene encoding hydrazine synthase was present in high abundance in the anoxic biofilms (1174 hits) and highly associated with *Candidatus Brocadia* (Fig. 5e). Furthermore, *Candidatus Brocadia* showed a strong association with the *hao*-like gene encoding hydroxylamine oxidoreductase (1944 hits), which is involved in the hydrazine synthesis through the hydroxylamine pathway. The abundant presence of these functional genes established a prerequisite for robust anammox metabolism at low temperatures and, more importantly, further evidenced the feasibility of enriching AnAOB with seasonal cooling. Interestingly, at the species level, AnAOB exhibited a high intraspecific diversity. Metagenomic sequencing identified 10 types of species belonging to *Candidatus Brocadia*, with the three most abundant being *Candidatus Brocadia sinica* (2260 reads), *Candidatus Brocadia pituitae* (1968 reads), and *Candidatus Brocadia sp. WS118* (950 reads) (Fig. 5f). Previous studies suggest that a functional community with higher intraspecific diversity generally exhibits greater adaptability when facing challenging conditions[39,40]. This may provide a microbiological explanation for the
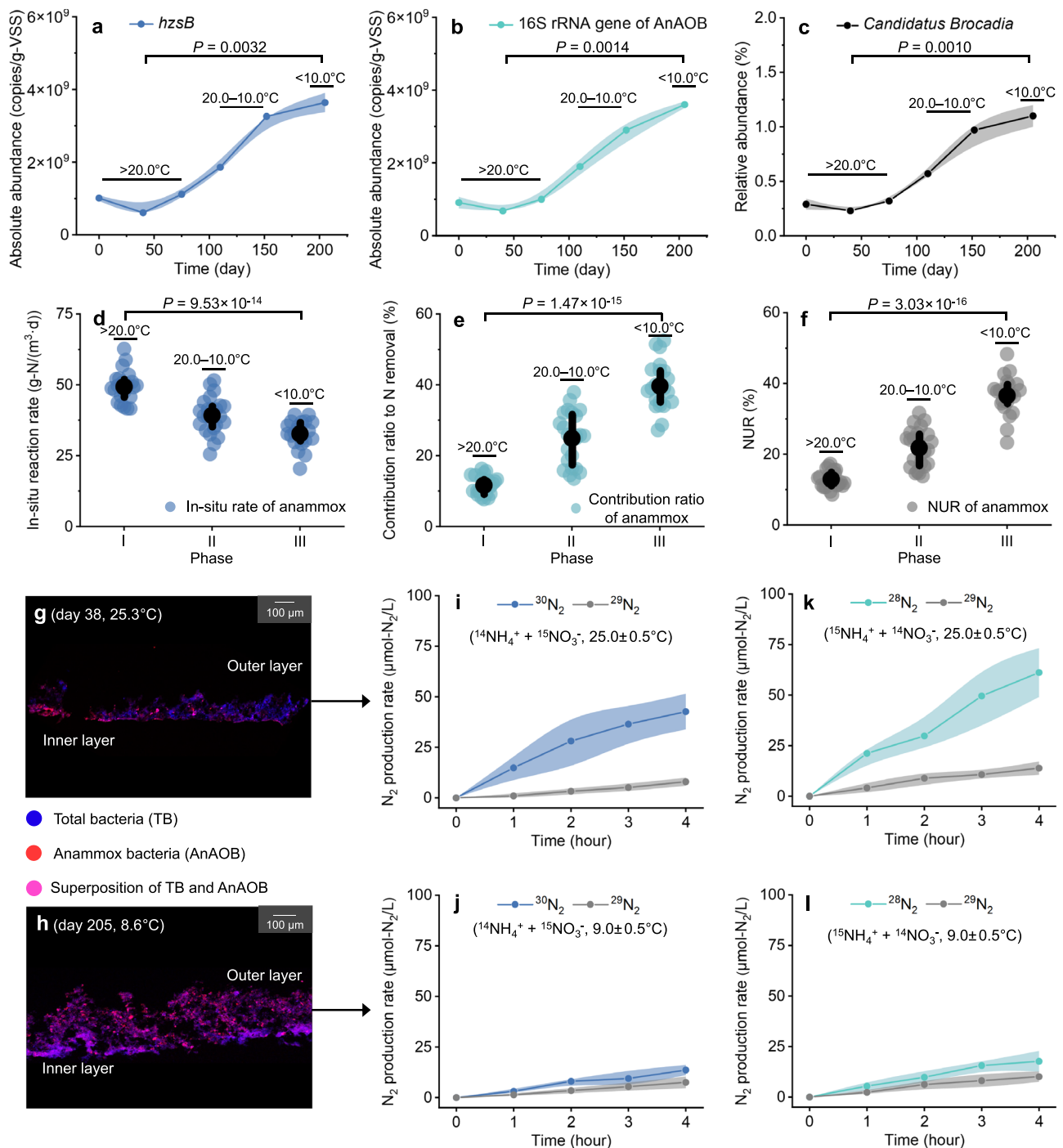
Fig. 3 | Long-term performance of mainstream anammox against seasonal cooling. a, b Absolute abundance of the anammox-specific *hzsB* gene and 16S rRNA gene by qPCR (*n* = 3 biologically independent samples, respectively), with two-tailed independent *t*-test showing the significance of inter-group differences. The error band represents the standard deviation (s.d.). Data are presented as mean ± s.d. **c** Relative abundance of *Candidatus Brocadia* by 16S rRNA amplicon sequencing (*n* = 2 biologically independent samples), with two-tailed independent *t*-test showing the significance of inter-group differences. The error band represents the s.d. Data are presented as mean ± s.d. **d–f** In-situ reaction rate of anammox in the anoxic zone, contribution ratio of anammox to total nitrogen removal, and NO_2^--utilizing ratio (NUR) of anammox in the anoxic zone, with two-tailed independent *t*-test showing the significance of inter-group differences. These anammox-related parameters were obtained from a total of 68 independent experiments (*n* = 68

independent experiments), including 23 from phase I, 24 from phase II, and 21 from phase III. The black circle represents the mean, and the black bar represents the quartile (25–75%) line. **g, h** Spatial distribution of anammox bacteria (AnAOB) within anoxic biofilms by confocal laser-scanning microscopy combining with fluorescence in situ hybridization (CLSM-FISH), with the second anoxic compartment as representative. Total bacteria (TB) and AnAOB exhibit blue (cy3) and red (cy5) fluorescence, respectively. Pink fluorescence results from the superposition of TB and AnAOB. ^{15}N stable isotope tracing tests experimental group at 25.0 ± 0.5 °C (**i**, samples from day 38) and 9.0 ± 0.5 °C (**j**, samples from day 205) (*n* = 3 independent experiments, respectively) and control group at 25.0 ± 0.5 °C (**k**, samples from day 38) and 9.0 ± 0.5 °C (**l**, samples from day 205) (*n* = 3 independent experiments, respectively). The error band represents the s.d. Data are presented as mean ± s.d. Source data are provided as a Source Data file.
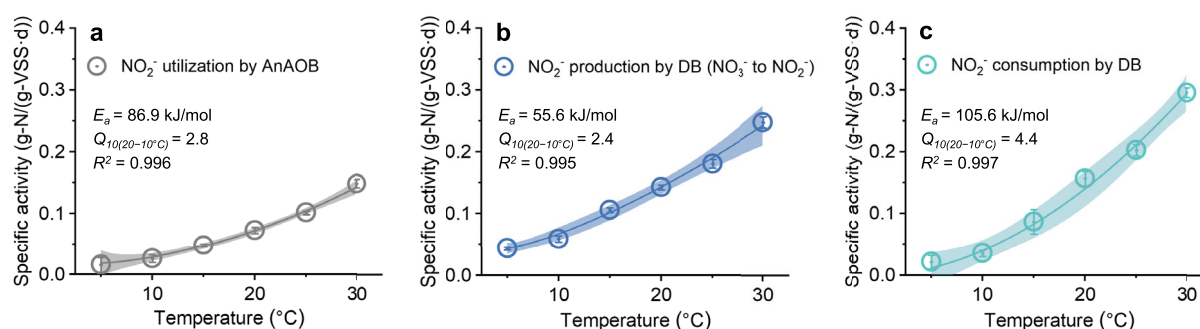
Fig. 4 | Temperature-dependent kinetic characteristics of the partial denitrification coupling with anammox (PDA) process in the temperature range from 30 °C to 5 °C based on the modified Arrhenius equation. a NO_2^- utilization by anammox bacteria (AnAOB). **b** NO_2^- production by denitrifying bacteria (DB) (NO_3^- to NO_2^-). **c** NO_2^- consumption by DB. All the tests were performed in triplicate ($n = 3$ independent experiments). The error bar represents the s.d. Data are presented as mean ± s.d. The background band represents the confidence interval (95%) in the fitting according to the modified Arrhenius equation. Source data are provided as a Source Data file.

successful retention and enrichment of AnAOB at low temperatures. Recent studies provided possible explanations for the advantage of *Candidatus Brocadia sinica* over other species. On the one hand, the transcriptional levels of functional genes involved in DNA replication, recombination, and repair, as well as inorganic ion transport and metabolism, could be upregulated to resist the cold. On the other hand, the cold shock proteins and cryoprotectants enhanced the low-temperature adaptability, particularly considering the upregulation of transcriptional levels of related functional genes with decreasing temperature[41,42].

Regarding the PD process, seasonal cooling shaped the cold-tolerant denitrifying populations. In the anoxic biofilms, *JG30-KF-CM45*, a typical cold-tolerant DB, significantly increased from 2.39% to 6.04% (Welch's two-tailed *t*-test, $P = 0.009$) (Fig. 5d). Additionally, *Candidatus Microthrix* and *Trichococcus*, both psychrophilic DBs, were highly enriched in the flocs, with relative abundances increasing from 2.03% to 6.30% (Welch's two-tailed *t*-test, $P < 0.001$) and from 1.75% to 4.08% (Welch's two-tailed *t*-test, $P = 0.035$), respectively (Fig. 5c). In contrast, traditional mesophilic DBs such as *OLB14* and *Saccharimonadales* significantly declined from 2.55% to 1.43% (Welch's two-tailed *t*-test, $P = 0.036$) and from 3.33% to 2.54% (Welch's two-tailed *t*-test, $P = 0.027$), respectively. Notably, at the species level, *Candidatus Microthrix parvicella* was detected in a high abundance (808 reads) in the flocs. Previous pure culture studies have revealed that *Candidatus Microthrix parvicella* (Bio17-1 genome) lacks the NO_2^- reductase[43], and the subsequent isotope labeling studies reconfirmed its ability to reduce NO_3^- to NO_2^- but not to reduce NO_2^- further[44,45]. These results unlock a new role for *Candidatus Microthrix parvicella* as the functional bacteria contributing to the PD process at low temperatures, which sheds fresh light on future research. On the one hand, strategically enriching *Candidatus Microthrix parvicella* under cold conditions may enable a more powerful NO_2^- supply to AnAOB; on the other hand, the negative impact of *Candidatus Microthrix parvicella*, as filamentous bacteria, on sludge settling must be weighed.

Discussion

PDA as an alternative for extending mainstream anammox towards non-tropical regions

From natural ecosystems to lab-scale tests and now to this pilot-scale plant, the low-temperature anammox has been progressively explored. Anammox has been acknowledged as a critical contributor to the nitrogen cycle in cold ecosystems, such as temperate freshwater lakes with annual mean temperatures below 15.0 °C and marine sediments ranging from 1.7 °C to 4.0 °C[46]. In lab-scale tests, AnAOB has been successfully cultured at low temperatures of 7.0 °C and 5.0 °C[33,47]. The mechanisms of AnAOB adapting to low-temperature conditions mainly involve the synthesis and secretion of various cold shock proteins (e.g., transcriptional regulators cold shock proteins A and B), protein chaperones (e.g., groEL/groES), RNA chaperones, and cryoprotectants (e.g., glycine betaine)[48,49]. Besides, the unique ladderane membrane lipids structure contributes to the low-temperature adaptability of AnAOB[49]. These findings suggest that AnAOB can adapt to a broad temperature range, bolstering confidence in extending mainstream anammox towards non-tropical regions. A stable NO_2^- supply for anammox across seasons is a prerequisite for this objective. Partial nitrification (PN) represents the best-known NO_2^- supplier for anammox (Supplementary Table 3). Compared to the nitrification-denitrification process, the PNA process technically reduces aeration consumption and organic carbon demand by up to 63% and 100%, respectively, offering significant sustainability and cost-effectiveness advantages[15,16]. For tropical and subtropical regions, the Changi water reclamation plant (200,000 m3/d) utilizing the step-feed PNA process has set a commendable precedent, playing a crucial role in the NEWater project of Singapore[50,51]. However, adopting the PNA process may be risky in non-tropical regions. From laboratory tests to full-scale applications, considerable evidence has demonstrated the high vulnerability of AOB to low temperatures compared to NOB, which complicates the suppression of NOB and poses a significant risk to NO_2^- supply[17,52]. Taking a full-scale WWTP in northern Israel (25,560 m3/d, A^2O process) as an example, the absolute abundance of NOB was over 100 times greater than that of AOB during low-temperature operations (13−20 °C), placing significant restrictions on the PN performance and AnAOB abundance[53].

For the first time, this pilot-scale plant evaluated the performance of mainstream PDA under real-world cold conditions. Compared to the nitrification-denitrification process, the PDA process technically reduces aeration consumption and organic carbon demand by 47% and 54%, respectively[16,54]. During long-term seasonal cooling, the NRE from actual municipal wastewater slightly decreased from 75.0 ± 4.6% (27.8−20.0 °C) to 70.4 ± 4.5% (10−7.5 °C) (Fig. 2c). In the absence of additional carbon source and tertiary (polishing) treatment, an NRE above 70% and an ARE above 99% at low temperatures below 10 °C surpassed most reported municipal wastewater treatment systems (typically, NRE below 60% and ARE below 95%)[25,55]. As a core contributor to nitrogen removal, the PDA process demonstrated remarkable low-temperature tolerance, with the in-situ anammox rate achieving 32.7 ± 4.7 g-N/(m³·d) at 10.0−7.5 °C, contributing 39.7 ± 6.7% to nitrogen removal (Fig. 3d−e). Additionally, AnAOB was successfully enriched in the anoxic biofilms with seasonal cooling, with absolute and relative abundances increasing by 429.1% and 343.5%, respectively (Fig. 3a−c). These results suggest that the PD process could not only contribute to the maintenance of anammox but also empower the thriving of anammox under real-world cold conditions, offering a
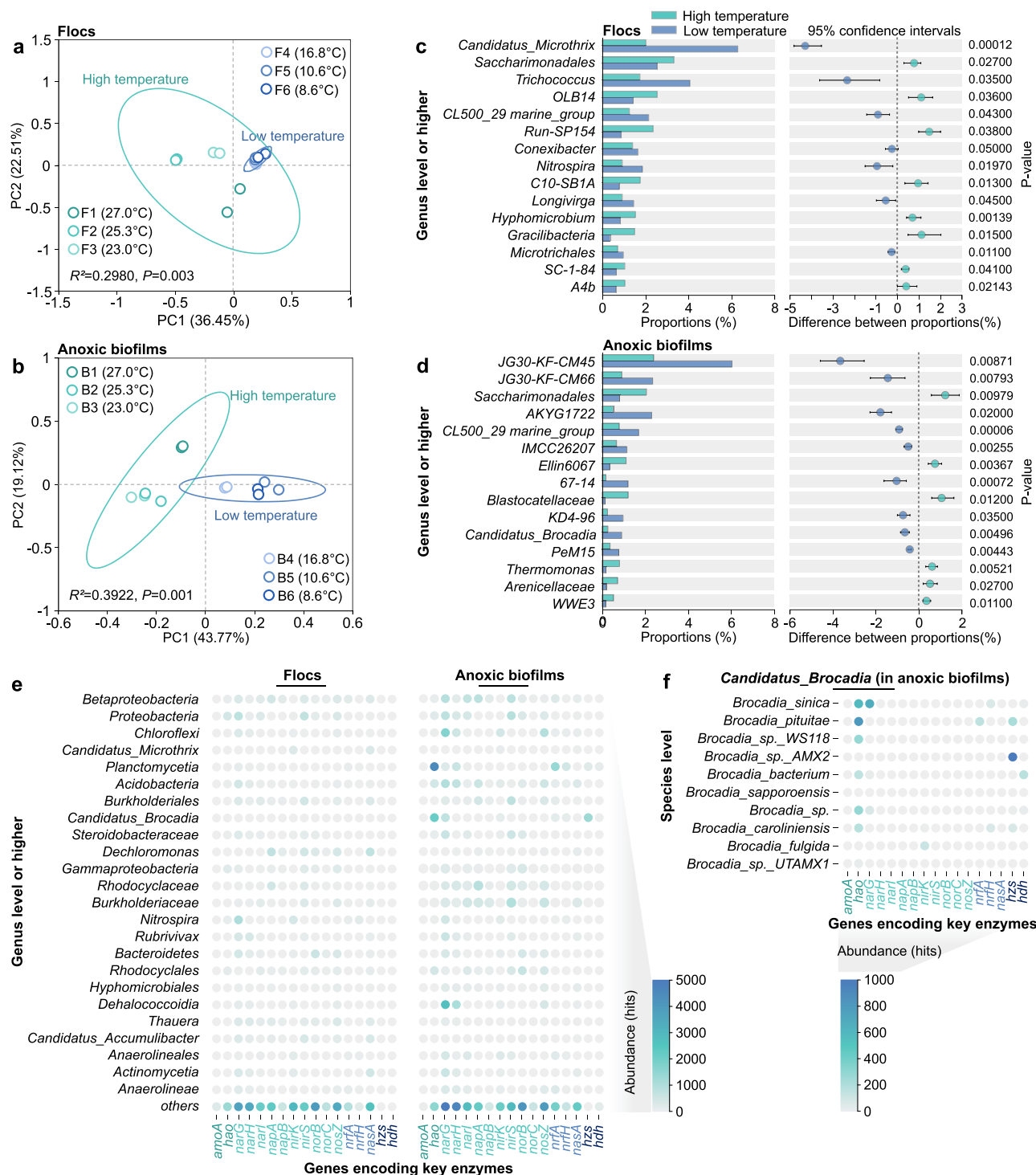
Fig. 5 | Dynamic succession of bacterial communities and taxonomic origins of key enzymes. a, b Principal coordinates analysis (PCoA) for flocs and anoxic biofilms at the operational taxonomic unit (OTU) level, with Adonis test showing the significance of inter-group differences. **c** Welch's two-tailed t-test bar plot for the core bacterial microbiome in the flocs at high and low temperatures ($n = 6$ biologically independent samples, respectively) at the genus level or higher. Dots in the right panel represent the differences in bacterial proportions. Error bars represent the 95% confidence intervals for the differences in bacterial proportions. **d** Welch's two-tailed t-test bar plot for the core bacterial microbiome in the anoxic biofilms at high and low temperatures ($n = 6$ biologically independent samples, respectively) at the genus level or higher. Dots in the right panel represent the differences in bacterial proportions. Error bars represent the 95% confidence intervals for the differences in bacterial proportions. **e** Taxonomic origins of key enzymes involved in nitrogen metabolism at the genus level or higher based on the Kyoto Encyclopedia of Genes and Genomes (KEGG) function database. **f** Taxonomy of *Candidatus Brocadia* at the species level and the origins of key enzymes involved in nitrogen metabolism based on the KEGG database. Source data are provided as a Source Data file.
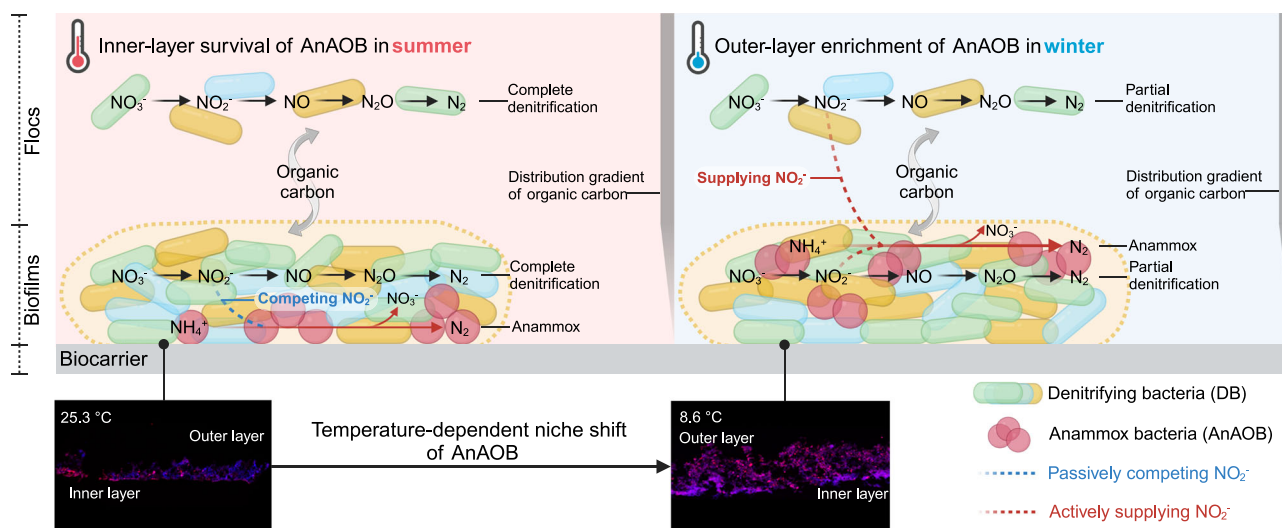
Fig. 6 | The proposed temperature-dependent niche model of anammox bacteria (AnAOB) presenting differences in the AnAOB niches during summer and winter in the hybrid process (flocs plus biofilms). The temperature-dependent transition from complete denitrification to partial denitrification, along with the spatial distribution gradient of organic carbon in the hybrid process (which positions flocs as hotspots for both complete and partial denitrification), potentially drives the shift of AnAOB niches. Figure 6 was created in BioRender. Zhao, Q. (2024) https://BioRender.com/w23o615.

promising alternative for extending mainstream anammox to non-tropical regions.

Opportunities and challenges for mainstream PDA

The encouraging results of this study prompt a reconsideration of the key factors contributing to the successful implementation of mainstream anammox under real-world cold conditions. Firstly, a sufficient NO_2^- supply from DB to AnAOB was a critical prerequisite. The residual NO_2^- in the anoxic zone during phase III (0.27 ± 0.15 mg-N/L in the fourth anoxic compartment, Supplementary Fig. 5) served as direct evidence of the sufficient NO_2^- supply, indicating a higher NO_2^- supply capacity of DB than the NO_2^- utilization capacity of AnAOB. In this sense, NO_2^- supply was no longer the rate-limiting step for mainstream anammox, as evidenced by both the in-situ and ex-situ data. The in-situ NUR of anammox was recorded at $36.6 \pm 5.4\%$ in phase III ($10-7.5\,^{\circ}\text{C}$) (Fig. 3f). Ex-situ kinetic tests with hybrid biomass (flocs plus anoxic biofilms) showed an NO_2^- accumulation ratio of approximately 40.1% at $10\,^{\circ}\text{C}$ (Fig. 4b–c). Previous studies have highlighted the dependency of AnAOB enrichment on a stable NO_2^- supply, exemplified by high AnAOB growth rates (e.g., 0.33 ± 0.02 d^{-1} and 0.18 d^{-1}) attained on the premise of sufficient NO_2^- availability[56,57]. Similar phenomena were observed in this pilot plant. Although higher temperatures inherently favored AnAOB, the complete denitrification mediated by DB limited the NO_2^- availability and impeded the AnAOB enrichment. As the operating temperature decreased, the NO_2^- supply capacity of DB was unlocked, thereby empowering the AnAOB enrichment. Comparing high and low temperatures suggests that within a certain temperature range (e.g., $5-30\,^{\circ}\text{C}$), a stable NO_2^- supply might be more indispensable for mainstream anammox than the temperature itself. This hypothesis explains why the correlation between the operating temperature and AnAOB abundance does not necessarily follow a positive trend[58]. Therefore, for non-tropical regions, it is essential not only to focus on the direct impact of temperature on AnAOB but also to consider the influence of temperature on NO_2^- supply and its indirect effect.

Secondly, effective attachment conditions are indispensable for mainstream anammox regardless of operating temperature. The long-term operation of this pilot plant reconfirmed the difficulty of maintaining an abundant anammox biomass within flocs. From summer to winter, the absolute abundance of AnAOB in the flocs remained below 1.0×10^7 copies/g-VSS (Supplementary Fig. 6), while that in the anoxic biofilms consistently exceeded 1.0×10^9 copies/g-VSS (Fig. 3a–b). Notably, our findings spotlight another implication of the attachment conditions: the biofilms offer a necessary platform for the adaptive niche shift of AnAOB during seasonal cooling. Specifically, at temperatures above $20\,^{\circ}\text{C}$, AnAOB primarily inhabited the inner layer of the anoxic biofilms, aligning with previous anoxic biofilm models[31,59,60]. In this study, the temperature-dependent kinetic characteristics of the PDA process offer a potential explanation for this pattern (Fig. 6). DB tends to complete denitrification without NO_2^- accumulation in the temperature range of $20-30\,^{\circ}\text{C}$ (NO_2^- production activity < NO_2^- consumption activity). From the perspective of organic carbon spatial distribution, flocs serve as hotspots for complete denitrification due to their direct exposure to organic carbon[61]. For the outer-layer biofilms, although the availability of organic carbon is lower compared to flocs due to mass transfer resistance, they still have advantages over the inner-layer biofilms[62,63]. Taken together, in the hybrid process (flocs plus biofilms), the availability of organic carbon forms a gradient from flocs to outer-layer biofilms and further to inner-layer biofilms (Fig. 6). Accordingly, DB exerts a stronger competitive selection pressure against AnAOB in the flocs and outer-layer biofilms, while the inner-layer biofilms provide a shelter for AnAOB, where a lower organic carbon level slows down complete denitrification and mitigates the competition from DB[60]. In this context, the preference of AnAOB for the inner-layer biofilms at higher temperatures may serve as a passive protection mechanism, potentially at the expense of decreases in AnAOB abundance (Fig. 3a–c). To test this hypothesis, we attempted to separate the inner and outer layers of the biofilms using a high-speed stirring method and evaluated the removal rate of NO_3^- and sCOD of the flocs, outer-layer biofilms, and inner-layer biofilms (Supplementary Fig. 7)[64]. The results yielded decreasing gradients (NO_3^- removal rate: 0.047 ± 0.005, 0.029 ± 0.012, and 0.017 ± 0.009 g-N/(g-VSS·d), respectively; sCOD removal rate: 0.281 ± 0.015, 0.147 ± 0.030, and 0.092 ± 0.014 g-O$_2$/(g-VSS·d), respectively), suggesting that differences in organic carbon levels shaped the denitrification capacity, thus supporting our hypothesis regarding the spatial distribution gradient of organic carbon. As the temperature decreased, the niche of AnAOB noticeably expanded towards the outer-layer biofilms. Notably, when testing flocs and biofilms separately at $10\,^{\circ}\text{C}$, the NO_2^- supply capacity of the flocs was significantly higher than that of the biofilms (0.021 ± 0.003 versus 0.006 ± 0.001 g-N/(g-VSS·d)) (Supplementary

Fig. 8), which partially reconfirms the hypothesis regarding the spatial distribution gradient of organic carbon and, more importantly, highlights that the flocs under cold conditions served as hotspots for the PD process. Consequently, the outer-layer biofilms, directly exposed to flocs, provided a more favorable niche for AnAOB to acquire NO_2^-, potentially driving its outward expansion. In this sense, biofilms diversified the niche options of AnAOB, enabling AnAOB to adapt to distinct microbial interaction patterns at different temperatures. Additionally, it is important to note that organic carbon may be a significant factor influencing the temperature-dependent niche shift of AnAOB. Specifically, along the anoxic zone, declines in the concentration and biodegradability of organic carbon resulted in decreased denitrification rates (Supplementary Fig. 5)[65]. Flocs, as hotspots for complete denitrification (at high temperatures) and PD (at low temperatures), are more directly impacted, resulting in a diminished inductive effect of flocs on the niche of AnAOB within the biofilms, as exemplified by the relatively slight niche changes of AnAOB observed in the fourth anoxic compartment (Supplementary Fig. 3). This diminishing was also reflected in the variations in AnAOB abundance. We compared the fluctuations in the AnAOB abundance in all four anoxic compartments using the coefficient of variation (CV). Both the CV of AnAOB abundance (0.73 to 0.55) and the sCOD removal rate (405.5 to 58.5 (g-O_2/m³·d)) exhibited a downward trend along the anoxic zone (Supplementary Fig. 9). These findings indicate that the impact of operating temperature on AnAOB varies spatially within the anoxic zone, and more practically, remind us that the concentration and biodegradability of organic carbon could serve as controllable parameters for managing the niche of AnAOB across different seasons.

Thirdly, the A^2O-BCO process provides a crucial safeguard for the robust PDA process. The A^2O-BCO is a modified version of the conventional A^2O process[66], which extends the anoxic zone of the A^2O unit and shortens the oxic zone[67]. On the one hand, the nitrification task is transferred to the BCO unit, not the oxic zone conventionally. The densely integrated biocarriers (providing sufficient sludge retention time for slow-growing AOB and NOB) and continuous aeration within the BCO unit contribute to stable nitrification[68]. In this pilot plant, the ARE reached up to 99.9 ± 0.3% at low temperatures of 10−7.5 °C, which not only enhanced the effluent quality of NH_4^+ but also ensured sufficient NO_3^- reflux into the anoxic zone as the substrate for the PDA process. Therefore, in the A^2O-BCO process, the nitrification crisis faced by conventional WWTPs at low temperatures will not become a limiting factor for the PDA process. On the other hand, the A^2O-BCO process allowed for an extended anoxic zone (constituting 52% of the total effective volume of this pilot plant), which enabled an expanded anammox footprint and amplified the anammox contribution to nitrogen removal.

This pilot-scale study sheds light on the feasibility of extending mainstream anammox towards non-tropical regions and, more importantly, indicates that there remains improvement room for mainstream PDA in future applications. In this pilot plant, the anammox contribution to nitrogen removal was 11.7 ± 2.5% in the summer and 39.7 ± 6.7% in the winter, effectively enhancing the nitrogen removal from municipal wastewater with a low C/N ratio (3.6 ± 0.7). However, it must be acknowledged that the current level of anammox contribution still falls short of expectations, particularly during the summer months. This shortfall was primarily due to two factors. Firstly, the absence of anammox bioaugmentation led to a limited AnAOB abundance, ranging from 0.23 ± 0.01% to 1.02 ± 0.10% in the anoxic biofilms. Secondly, this pilot plant lacked flexible operational strategies to promote the synergy between DB and AnAOB across different seasons. A similar predicament was observed at the Xi'an NO. 4 WWTP in northern China (250,000 m3/d, A^2O process), whose anammox contribution ratio has struggled to surpass 20% during summer operations[25]. Our results offer insights into the predicament encountered by mainstream PDA during the summer months. On the one hand, at high temperatures above 20 °C, the primary interaction between DB and AnAOB is competitive for NO_2^- rather than cooperative in NO_2^- supply. On the other hand, the biomass of heterotrophic DB generally far exceeds that of autotrophic AnAOB, exacerbating the competitive selection pressure suffered by the latter[60]. Recent years have witnessed strategies for mainstream PDA enhancement by encouraging NO_2^- accumulation by DB, such as adding readily biodegradable organic carbon sources (e.g., sodium acetate and glucose) and strategically controlling the C/N ratio[29,69,70]. Yet, regrettably, these optimal conditions are often lacking in WWTPs, as exemplified by the Xi'an NO. 4 WWTP and the Wuqing WWTP in Tianjin, China (30,000 m3/d, oxidation ditch process)[6,25]. The most recent study has introduced a biomass concentration management as a technically accessible strategy to mitigate the competition of DB against AnAOB[31,59]. Taking the hybrid process as an example, lowering the flocs concentration can effectively diminish the DB biomass without affecting the AnAOB biomass (primarily inhabiting biofilms), which narrows the biomass disparity between DB and AnAOB and balances their competition for NO_2^-. As reported, the biomass concentration management facilitated a remarkable anammox contribution ratio (above 50%) at 24.0 ± 2.2 °C, accompanied by a high-level enrichment of AnAOB in the biofilms (relative abundance above 5.0%)[60]. The strategic biomass concentration down-regulation offers a promising solution to the challenges faced by mainstream PDA during summer operations. Meanwhile, it reminds us that under cold conditions, up-regulating the flocs concentration can be employed to enhance the NO_2^- supply from flocs to biofilms, thereby maximizing the anammox contribution and AnAOB enrichment. Compared to other existing strategies, managing biomass concentration flexibly, based on the distinct interactions between DB and AnAOB in different seasons, is more engineering-friendly and sustainable. Based on this conceptual framework, we hope mainstream PDA empowers sustainable nitrogen removal in non-tropical regions across seasons, thereby contributing to the global resolution of the Water-Energy-Sanitation crisis.

Methods

Designing, operating, and monitoring of the pilot plant

The pilot-scale plant of the A^2O-BCO process was installed at the R&D center of Shahe reclaimed municipal wastewater treatment plant in Beijing, China, with a treatment capacity of 50 m3/day. Raw municipal wastewater was sourced from a full-scale aerated grit chamber. The pilot plant consisted of three core structures: A^2O unit (24.0 m³), vertical-flow settler (6.0 m³), and BCO unit (6.8 m³) (Fig. 1). The A^2O unit was composed of six rectangular-shaped compartments (one anaerobic, four anoxic, and one oxic), each with an effective volume of 4.0 m³ (length × width × depth = 1.0 × 1.0 × 4.0 m). The cylindrical polypropylene biocarriers (K3, Yulong, China) were integrated into the anoxic zones at a volumetric packing ratio of 16% (Supplementary Table 4). Submersible stirring impellers (FSJ, Nuoli, China) were fitted in each compartment to ensure homogenization. The effluent of the A^2O was gravitationally directed into the vertical-flow settler. The supernatant flowed over the weirs and was pumped into the cylinder-shaped BCO unit (diameter × depth=1.2 × 6.0 m). The nitrifying bacteria-containing biocarriers (K3, Yulong, China) were integrated into the BCO unit at a volumetric packing ratio of 55%.

The pilot plant was automated with a programmable logic controller (PLC) system (Supplementary Fig. 10). An online monitoring apparatus (MIQ/TC 2020 3 G, WTW, Germany) was installed to monitor the real-time fluctuation of NH_4^+ and NO_3^- in influent and effluent. Multiparameter probes (Multi 3420, WTW, Germany) were used to monitor the DO, pH, and operating temperature. DO concentrations were maintained at 0.58 ± 0.36 mg-O_2/L in the oxic zone and 2.04 ± 0.64 mg-O_2/L in the BCO unit (Supplementary Figs. 11 and 12). The sludge reflux ratio and nitrifying liquid reflux ratio were set to 100% and 200%, respectively. The total effective hydraulic retention

time (HRT) was 14.8 h (11.5 h for the A^{2}O and 3.3 h for the BCO). The sludge retention time (SRT) of the flocs in the A^{2}O unit was approximately 15–20 days. The mixed liquor volatile suspended solid (MLVSS) was 2223 ± 303 mg/L (Supplementary Fig. 13). The average biomass per anoxic biocarrier was 53.5 ± 2.8 mg, corresponding to 856.4 ± 44.4 mg-VSS/L; the average biomass per BCO biocarrier was 33.6 ± 1.3 mg, corresponding to 1846.2 ± 73.5 mg-VSS/L (Supplementary Fig. 14).

Analytical methods

Wastewater samples were collected from the pilot plant on a bi-daily basis, filtered through qualitative filter papers with a 15–20 μm pore size (NEWSTAR, China), and analyzed immediately. A Lachat Quik Chem 8500 Flow Injection Analyzer (Lachat Instruments, USA) was used to determine the concentrations of NH_4^+, NO_2^-, NO_3^-, and PO_4^{3-}. A Lian-hua 5B-1 quick-analysis apparatus (Lian-hua Tech, China) was used to determine the concentration of sCOD. According to the manufacturer's protocol, the wastewater sample was re-filtered through the 0.45 μm membrane filters (Jingteng, China) before testing for sCOD. A prepASH 340 series automatic moisture and ash analyzer (Precisa Gravimetrics AG, Switzerland) was employed to determine the total suspended solids (TSS) and volatile suspended solids (VSS) of the flocs and biofilms.

^{15}N stable isotope tracing tests

On days 38 (25.3 °C) and 205 (8.6 °C), the flocs and biofilms were harvested from the second anoxic compartment, rinsed with ultrapure water, and flushed with helium gas (He, 99.999 vol%, Huayuchen, China) for 10 minutes. The sludge samples were then transferred into headspace incubation vials with an effective volume of 12 mL (Exetainer, Labco, UK). On day 38, the final biomass concentrations of the flocs and biofilms (volumetric packing ratio of 16%) were recorded as 2303.1 ± 101.2 and 1015.8 ± 152.2 mg-VSS/L, respectively. On day 205, the final biomass concentrations of flocs and biofilms were 1919.5 ± 86.2 and 922.3 ± 106.5 mg-VSS/L, respectively. Two types of ^{15}N-amended stock solutions were used for the tracing tests: $^{14}NH_4^+$ plus $^{15}NO_3^-$ (experimental group, 10.0 mg-N/L final concentration each) and $^{15}NH_4^+$ plus $^{14}NO_3^-$ (control group, 10.0 mg-N/L final concentration each) (Cambridge Isotope Laboratories, Inc., USA)[71]. The incubations were conducted in thermostatic incubators (HT-600B, Spring Instrument, China) at 25.0 ± 0.5 °C (day 38) and 9.0 ± 0.5 °C (day 205), respectively. The incubations were terminated at various times (0 h, 1 h, 2 h, 3 h, and 4 h) by injecting $ZnCl_2$ solution (200 μL, 7.0 M)[72]. The resulting $^{28}N_2$, $^{29}N_2$, and $^{30}N_2$ gases were determined using an isotope ratio mass spectrometer (253 Plus, Thermo, Germany).

Ex-situ kinetic tests

Ex-situ kinetic tests were conducted in serum bottles with an effective volume of 0.5 L, as detailed in Supplementary Table 5. Before testing, sludge samples were collected from the second anoxic compartment, rinsed with ultrapure water, and transferred into the serum bottles. All test groups were subjected to the same biomass conditions: flocs (2070.2 ± 102.3 mg-VSS/L) and anoxic biofilms (volumetric packing ratio of 16%, corresponding to 902.3 ± 53.4 mg-VSS/L). The mixed gas of nitrogen (N_2, 95.0 vol%) and carbon dioxide (CO_2, 5.0 vol%) (Huayuchen, China) was injected into the serum bottles until the DO concentration fell below 0.02 mg-O_2/L. Substrates, mineral substances, and trace elements were added to the serum bottles through a sealed pipe (Supplementary Table 6). The serum bottles were placed in a thermostatic water bath shaker (100 RPM) to control the testing temperature and ensure homogenization. At appropriate time intervals, 5 mL of the suspensions were extracted through a sealed pipe, filtered through qualitative filter papers with a 15–20 μm pore size, sealed, and analyzed.

Microbiological analysis

Samples of flocs and anoxic biofilms were collected from all four anoxic compartments at days 1 (27.0 °C), 38 (25.3 °C), 75 (23.0 °C), 110

(16.8 °C), 152 (10.6 °C), and 205 (8.6 °C). The samples were immediately freeze-dried using Labconco Free Zone 2.0 (Labconco, USA). DNA extraction was conducted using the Fast DNA Spin kits for soil (Bio 101, Vista, USA), and DNA concentration was measured using a NanoDrop 1000 spectrophotometer (NanoDrop Technologies, USA). The absolute abundances of the anammox-specific *hzsB* gene and 16S rRNA gene were determined using a qPCR thermocycler (Stratagene MX3000P, USA) with the fluorescent dye of SYBR-Green (TaKaRa, China). Information on primer pairs and thermal programs is detailed in Supplementary Table 7.

Samples of flocs and anoxic biofilms were collected from the second anoxic compartment at days 1, 38, 75, 110, 152, and 205 for high-throughput 16S rRNA amplicon sequencing. PCR amplification was conducted on bacterial 16S rRNA genes using primer pair 338 F and 806 R targeting the V3 and V4 hypervariable regions. Amplicon sequencing was performed on the Illumina Miseq platform at Majorbio Bio-Pharm Technology Co. Ltd. (Shanghai, China). Samples of flocs and anoxic biofilms were collected from the second anoxic compartment on day 205 for metagenomic sequencing. The paired-end sequencing was conducted on the HiSeq4000 platform (Illumina Inc., USA) by Majorbio Bio-Pharm Technology Co. Ltd. (Shanghai, China) with HiSeq 3000/4000 SBS kits. Detailed processing and analyzing procedures for high-throughput 16S rRNA amplicon sequencing and metagenomic sequencing are presented in Supplementary Notes 5 and 6. Raw sequencing data are available in NCBI Sequence Read Archive (SRA) with the accession codes PRJNA793238 and PRJNA1166713.

Anoxic biofilms were harvested from all four anoxic compartments on days 38 (25.3 °C) and 205 (8.6 °C) for CLSM-FISH analysis. The sequences of the oligonucleotide probes (AMX 368, EUB 338 I, EUB 338 II, and EUB 338 III) and the sampling processes are detailed in Supplementary Note 7.

Statistical analysis

The mean values, standard deviations, two-tailed paired *t*-tests, and two-tailed independent *t*-tests were performed in GraphPad Prism (Version 8.0). The Welch's two-tailed *t*-test was performed in STAMP (Version 2.1.3). The Adonis test was performed on Majorbio Cloud (www.i-sanger.com). The significance level was to α = 0.05 (*P* value ≤ 0.05).

Reporting summary

Further information on research design is available in the Nature Portfolio Reporting Summary linked to this article.

Data availability

The data generated in this study are provided within the paper, Supplementary Information. Raw sequencing data are available in NCBI Sequence Read Archive (SRA) with the accession codes PRJNA793238 and PRJNA1166713. Source data are provided with this paper.

References

1. Naddaf, M. The world faces a water crisis-4 powerful charts show how. *Nature* **615**, 774–775 (2023).
2. Grego, S. The humble toilet is an opportunity for sustainable water reuse. *Nat. Water* **1**, 900–901 (2023).
3. Tortajada, C. Reused water as a source of clean water and energy. *Nat. Water* **2**, 102–103 (2024).
4. Sachs, J. D. et al. Six transformations to achieve the Sustainable Development Goals. *Nat. Sustain.* **2**, 805–814 (2019).
5. Du, W. et al. Spatiotemporal pattern of greenhouse gas emissions in China's wastewater sector and pathways towards carbon neutrality. *Nat. Water* **1**, 166–175 (2023).
6. Liu, X. et al. Achieving and control of partial denitrification in anoxic-oxic process of real municipal wastewater treatment plant. *Bioresour. Technol.* **341**, 125765 (2021).

7. Shen, N. & Zhou, Y. Enhanced biological phosphorus removal with different carbon sources. *Appl. Microbiol. Biotechnol.* **100**, 4735–4745 (2016).

8. Li, P. et al. Tertiary nitrogen removal for municipal wastewater using a solid-phase denitrifying biofilter with polycaprolactone as the carbon source and filtration medium. *Water Res* **93**, 74–83 (2016).

9. Lotti, T., Kleerebezem, R., Lubello, C. & van Loosdrecht, M. C. M. Physiological and kinetic characterization of a suspended cell anammox culture. *Water Res* **60**, 1–14 (2014).

10. Kuenen, J. G. Anammox bacteria: from discovery to application. *Nat. Rev. Microbiol.* **6**, 320–326 (2008).

11. Cao, Y. et al. The influence of dissolved oxygen on partial nitration/anammox performance and microbial community of the 200,000 m³/d activated sludge process at the Changi water reclamation plant (2011 to 2016). *Water Sci. Technol.* **78**, 634–643 (2018).

12. Huang, X. et al. C-N-S synergy in a pilot-scale mainstream anammox fluidized-bed membrane bioreactor for treating chemically enhanced primary treatment saline sewage. *Water Res* **229**, 119475 (2023).

13. Nawaz, A. et al. Intelligent Human–Machine Interface: An agile operation and decision support for an ANAMMOX SBR system at a pilot-scale wastewater treatment plant. *Ieee Trans. Ind. Inform.* **18**, 6224–6232 (2022).

14. Laureni, M. et al. Mainstream partial nitration and anammox: long-term process stability and effluent quality at low temperatures. *Water Res* **101**, 628–639 (2016).

15. Qiu, S. et al. What's the best way to achieve successful mainstream partial nitrification-anammox application? *Crit. Rev. Environ. Sci. Technol.* **51**, 1045–1077 (2021).

16. Zhao, Q. et al. Sustainable upgrading of biological municipal wastewater treatment based on anammox: From microbial understanding to engineering application. *Sci. Total Environ.* **813**, 152468 (2022).

17. Trojanowicz, K., Trela, J. & Plaza, E. Possible mechanism of efficient mainstream partial nitration/anammox (PN/A) in hybrid bioreactors (IFAS). *Environ. Technol.* **42**, 1023–1037 (2021).

18. Akaboci, T. R. V., Gich, F., Ruscalleda, M., Balaguer, M. D. & Colprim, J. Assessment of operational conditions towards mainstream partial nitration-anammox stability at moderate to low temperature: Reactor performance and bacterial community. *Chem. Eng. J.* **350**, 192–200 (2018).

19. Gong, X. et al. Performance of the anammox process treating low-strength municipal wastewater under low temperatures: Effect of undulating seasonal temperature variation. *Bioresour. Technol.* **312**, 123590 (2020).

20. Du, R., Cao, S., Peng, Y., Zhang, H. & Wang, S. Combined Partial Denitrification (PD)-Anammox: A method for high nitrate wastewater treatment. *Environ. Int.* **126**, 707–716 (2019).

21. Wang, D., Luo, Q., Huang, K. & Zhang, X. Distinct mechanisms underlying assembly processes and interactions of microbial communities in two single-stage bioreactors coupling anammox with denitrification. *Chem. Eng. J.* **452**, 139319 (2023).

22. Ma, B., Qian, W., Yuan, C., Yuan, Z. & Peng, Y. Achieving Mainstream Nitrogen Removal through Coupling Anammox with Denitratation. *Environ. Sci. Technol.* **51**, 8405–8413 (2017).

23. Du, R., Cao, S., Zhang, H., Li, X. & Peng, Y. Flexible nitrite supply alternative for mainstream anammox: advances in enhancing process stability. *Environ. Sci. Technol.* **54**, 6353–6364 (2020).

24. Zhao, Q. et al. Pilot-scale evaluation of partial denitrification/anammox on nitrogen removal from low COD/N real sewage based on a modified process. *Bioresour. Technol.* **338**, 125580 (2021).

25. Li, J. et al. Quantify the contribution of anammox for enhanced nitrogen removal through metagenomic analysis and mass balance in an anoxic moving bed biofilm reactor. *Water Res* **160**, 178–187 (2019).

26. Wang, D., He, Y. & Zhang, X. A comprehensive insight into the functional bacteria and genes and their roles in simultaneous denitrification and anammox system at varying substrate loadings. *Appl. Microbiol. Biotechnol.* **103**, 1523–1533 (2019).

27. Du, R. et al. Beyond an applicable rate in low-strength wastewater treatment by anammox: motivated labor at an extremely short hydraulic retention time. *Environ. Sci. Technol.* **56**, 8650–8662 (2022).

28. Xu, A. et al. A novel process of salt tolerance partial denitrification and anammox (ST-PDA) for treating saline wastewater. *Bioresour. Technol.* **345**, 126472 (2022).

29. Zhang, M. et al. Nitrite accumulation and microbial behavior by seeding denitrifying phosphorus removal sludge for partial denitrification (PD): The effect of COD/NO₃⁻ ratio. *Bioresour. Technol.* **323**, 124524 (2021).

30. Qian, W., Ma, B., Li, X., Zhang, Q. & Peng, Y. Long-term effect of pH on denitrification: High pH benefits achieving partial-denitrification. *Bioresour. Technol.* **278**, 444–449 (2019).

31. Li, J. et al. Highly enriched anammox within anoxic biofilms by reducing suspended sludge biomass in a real-sewage A²/O process. *Water Res. (Oxf.).* **194**, 116906 (2021).

32. Kosgey, K. et al. Critical analysis of biomass retention strategies in mainstream and sidestream ANAMMOX-mediated nitrogen removal systems. *Environ. Sci. Technol.* **55**, 9–24 (2021).

33. Song, Y. et al. Architecture of HAP-anammox granules contributed to high capacity and robustness of nitrogen removal under 7 °C. *Water Res* **206**, 117764 (2021).

34. Park, G., Takekawa, M., Soda, S., Ike, M. & Furukawa, K. Temperature dependence of nitrogen removal activity by anammox bacteria enriched at low temperatures. *J. Biosci. Bioeng.* **123**, 505–511 (2017).

35. Jéglot, A., Sørensen, S. R., Schnorr, K. M., Plauborg, F. & Elsgaard, L. Temperature sensitivity and composition of nitrate-reducing microbiomes from a full-scale woodchip bioreactor treating agricultural drainage water. *Microorganisms* **9**, 1331 (2021).

36. Vacková, L., Srb, M., Stloukal, R. & Wanner, J. Comparison of denitrification at low temperature using encapsulated Paracoccus denitrificans, Pseudomonas fluorescens and mixed culture. *Bioresour. Technol.* **102**, 4661–4666 (2011).

37. Chen, D. et al. Controlling denitrification accompanied with nitrite accumulation at the sediment-water interface. *Ecol. Eng.* **100**, 194–198 (2017).

38. Shen, Q. et al. The influence mechanism of temperature on solid phase denitrification based on denitrification performance, carbon balance, and microbial analysis. *Sci. Total Environ.* **732**, 139333 (2020).

39. Govaert, L., Hendry, A. P., Fattahi, F. & Möst, M. Quantifying interspecific and intraspecific diversity effects on ecosystem functioning. *Ecology* **105**, (2024).

40. Kelvin, L. K. et al. Interspecific diversity reduces and functionally substitutes for intraspecific variation in biofilm communities. *Isme J.* **10**, 846–857 (2016).

41. Huang, K. et al. Temporal differentiation in the adaptation of functional bacteria to low-temperature stress in partial denitrification and anammox system. *Environ. Res.* **244**, 117933 (2024).

42. Okabe, S., Shafdar, A. A., Kobayashi, K., Zhang, L. & Oshiki, M. Glycogen metabolism of the anammox bacterium "Candidatus Brocadia sinica". *Isme J.* **15**, 1287–1301 (2021).

43. Muller, E. E. L. et al. Genome sequence of "Candidatus Microthrix parvicella" Bio17-1, a long-chain-fatty-acid-accumulating filamentous actinobacterium from a biological wastewater treatment plant. *J. Bacteriol.* **194**, 6670–6671 (2012).

44. Fan, N., Qi, R., Huang, B., Jin, R. & Yang, M. Factors influencing Candidatus Microthrix parvicella growth and specific filamentous bulking control: A review. *Chemosphere* **244**, 125371 (2020).

45. McIlroy, S. J. et al. Metabolic model for the filamentous 'Candidatus Microthrix parvicella' based on genomic and metagenomic analyses. *Isme J*. **7**, 1161–1172 (2013).

46. Zhou, S., Borjigin, S., Riya, S., Terada, A. & Hosomi, M. The relationship between anammox and denitrification in the sediment of an inland river. *Sci. Total Environ*. **490**, 1029–1036 (2014).

47. Kouba, V. et al. Adaptation of anammox bacteria to low temperature via gradual acclimation and cold shocks: Distinctions in protein expression, membrane composition and activities. *Water Res* **209**, 117822 (2022).

48. Frank, J. et al. Resolving the complete genome of Kuenenia stuttgartiensis from a membrane bioreactor enrichment using Single-Molecule Real-Time sequencing. *Sci Rep*. **8**, (2018).

49. Kouba, V., Bachmannová, C., Podzimek, T., Lipovová, P. & van Loosdrecht, M. C. M. Physiology of anammox adaptation to low temperatures and promising biomarkers: A review. *Bioresour. Technol*. **349**, 126847 (2022).

50. Cao, Y. et al. The occurrence of enhanced biological phosphorus removal in a 200,000 m^3/day partial nitration and Anammox activated sludge process at the Changi water reclamation plant. *Singap. Water Sci. Technol*. **75**, 741–751 (2017).

51. Lefebvre, O. Beyond NEWater: An insight into Singapore's water reuse prospects. *Curr. Opin. Environ. Sci. Health* **2**, 26–31 (2018).

52. Wett, B. et al. Going for mainstream deammonification from bench to full scale for maximized resource efficiency. *Water Sci. Technol*. **68**, 283–289 (2013).

53. Nejidat, A. et al. Abundance and diversity of anammox bacteria in a mainstream municipal wastewater treatment plant. *Appl. Microbiol. Biotechnol*. **102**, 6713–6723 (2018).

54. Zhang, M., Wang, S., Ji, B. & Liu, Y. Towards mainstream deammonification of municipal wastewater: Partial nitrification-anammox versus partial denitrification-anammox. *Sci. Total Environ*. **692**, 393–401 (2019).

55. Zhou, H., Li, X., Xu, G. & Yu, H. Overview of strategies for enhanced treatment of municipal/domestic wastewater at low temperature. *Sci. Total Environ*. **643**, 225–237 (2018).

56. Lotti, T., Kleerebezem, R., Abelleira-Pereira, J. M., Abbas, B. & van Loosdrecht, M. C. M. Faster through training: The anammox case. *Water Res* **81**, 261–268 (2015).

57. Zhang, L. et al. Maximum specific growth rate of anammox bacteria revisited. *Water Res* **116**, 296–303 (2017).

58. Lotti, T., Kleerebezem, R. & van Loosdrecht, M. C. M. Effect of temperature change on anammox activity. *Biotechnol. Bioeng*. **112**, 98–103 (2015).

59. Liu, Q. et al. Mechanism of suspended sludge impact on anammox enrichment in anoxic biofilm through long term operation and microbial analysis. *Water Res* **229**, 119412 (2023).

60. Zhao, Q. et al. From hybrid process to pure biofilm anammox process: Suspended sludge biomass management contributing to high-level anammox enrichment in biofilms. *Water Res* **236**, 119959 (2023).

61. Shao, Y., Shi, Y., Mohammed, A. & Liu, Y. Wastewater ammonia removal using an integrated fixed-film activated sludge-sequencing batch biofilm reactor (IFAS-SBR): Comparison of suspended flocs and attached biofilm. *Int. Biodeterior. Biodegrad*. **116**, 38–47 (2017).

62. Liu, Y., Li, C., Lackner, S., Wagner, M. & Horn, H. The role of interactions of effective biofilm surface area and mass transfer in nitrogen removal efficiency of an integrated fixed-film activated sludge system. *Chem. Eng. J. (Lausanne, Switz.: 1996)*. **350**, 992–999 (2018).

63. Nogueira, B. L. et al. Determination of the external mass transfer coefficient and influence of mixing intensity in moving bed biofilm reactors for wastewater treatment. *Water Res* **80**, 90–98 (2015).

64. Liu, C. et al. Rapid formation of granules coupling n-DAMO and anammox microorganisms to remove nitrogen. *Water Res* **194**, 116963 (2021).

65. Zhao, Q. et al. Carbon-restricted anoxic zone as an overlooked anammox hotspot in municipal wastewater treatment plants. *Environ. Sci. Technol*. **57**, 21767–21778 (2023).

66. Chen, Y. et al. Effect of nitrate recycling ratio on simultaneous biological nutrient removal in a novel anaerobic/anoxic/oxic (A^2/O)-biological aerated filter (BAF) system. *Bioresour. Technol*. **102**, 5722–5727 (2011).

67. Sun, Y., Zhang, L., Peng, Y., Chen, Y. & Lin, Y. Response of a novel denitrifying phosphorus removal (AAO-BCO) system to sinusoidal flow perturbation of municipal sewage: Adaptability, tolerance and improvement. *Sci. Total Environ*. **904**, 165837 (2023).

68. Zhang, M. et al. Organic substrate transformation and sludge characteristics in the integrated anaerobic anoxic oxic–biological contact oxidation (A^2/O–BCO) system treating wastewater with low carbon/nitrogen ratio. *Chem. Eng. J*. **283**, 47–57 (2016).

69. Li, J. et al. Enhanced nitrogen removal assisted by mainstream partial-anammox from real sewage in a continuous flow A^2/O reactor. *Chem. Eng. J*. **400**, 125893 (2020).

70. Ali, P. et al. Primary sludge fermentate as carbon source for mainstream partial denitrification–anammox (PdNA). *Water Environ. Res*. **93**, 1044–1059 (2021).

71. Zhu, G. et al. Hotspots of anaerobic ammonium oxidation at land–freshwater interfaces. *Nat. Geosci*. **6**, 103–107 (2013).

72. Marchant, H. K., Mohr, W. & Kuypers, M. M. Recent advances in marine N-cycle studies using 15N labeling methods. *Curr. Opin. Biotechnol*. **41**, 53–59 (2016).

Acknowledgements

Author contributions
The project was conceived and led by L.Z. and Y.P. Q.Z., J.L., T.J., and Q.Zhang contributed to the chemical, microbial, and statistical analysis. Q.Z. and L.Z. wrote the manuscript, and Y.P. significantly contributed by commenting upon and revising it. All authors discussed and interpreted the results and contributed to the manuscript.

Competing interests
The authors declare no competing interests.

Additional information
Supplementary information The online version contains supplementary material available at https://doi.org/10.1038/s41467-024-54805-x.

Correspondence and requests for materials should be addressed to Liang Zhang.

Peer review information *Nature Communications* thanks Alba Pedrouso Fuentes, Tommaso Lotti and the other, anonymous, reviewer(s) for their contribution to the peer review of this work. A peer review file is available.

Reprints and permissions information is available at http://www.nature.com/reprints

Publisher's note Springer Nature remains neutral with regard to jurisdictional claims in published maps and institutional affiliations.